DESIGN OF A NEW EMITTANCE METER FOR LINAC4

B. Cheymol, E. Bravin, C. Dutriat, T. Lefevre, CERN, Geneva, Switzerland

Abstract

LINAC4 is the first step in the upgrade of the injectors chain of the Large Hadron Collider (LHC). This Linac will accelerate H⁻ ions from 45 keV to 160 MeV. During the commissioning phase of LINAC4 transverse emittance measurements will be required at 45 keV, 3 MeV and 12 MeV. For this purpose a slit&grid system is currently being developed. The material and the geometry of the wires and of the slit need to be optimized in order to minimize the negative effects of the energy deposition and maximize the signals. This document describes the results of the studies carried out during the design of the emittance meter.

LINAC4

LINAC4 is an H⁻ linear accelerator with a maximum energy of 160 MeV intended to replace the present 50 MeV proton linac (LINAC2) as injector for the Proton Synchrotron Booster (PSB). In the present configuration the PSB represents the bottleneck in terms of beam brightness for the LHC. By injecting into the PSB a beam of higher energy and by using the phase-space painting technique, possible thanks to the use of H⁻ ions, the brightness and intensity of the beams produced by the PSB will double. In order to push the performances of the LHC even further additional upgrades of the injectors are foreseen. In the second step both the PSB and the Proton synchrotron (PS) will be replaced by a superconducting proton linac (SPL) and a new proton synchrotron, the PS2. [1]

EMITTANCE MESSUREMENT

The transverse phase-spaces (x and y) describe the distribution of particles in x and x' (y and y'), where x (y) is the position of the particles and x' (y') the angle between the trajectory of the particle and the longitudinal axis of the beam (z). The aim of the emittance meter is to sample the transverse phase-spaces from which the emittance can be calculated.
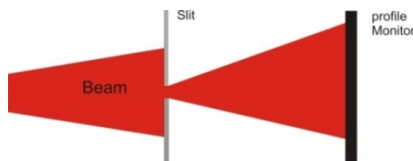

Figure 1: Slit and grid system.

As show in Fig. 1 and Fig. 2 a slit and grid system can be used to sample the transverse phase-space. In this technique the slit is used to select particles within a narrow slice in position, then, in the following drift space, the angular distribution of the particles transmitted through the slit is transformed into a position distribution and sampled using a profile monitor, in our case a secondary emission grid. By scanning the slit across the beam, the whole phase-space is reconstructed.
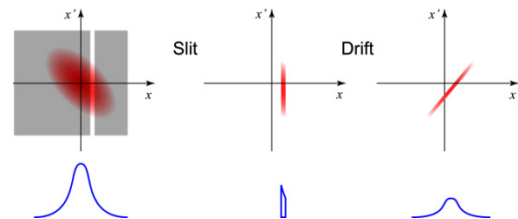

Figure 2: Phase-space sampling using a slit and grid system.

Each wire of the grid is connected to a separate acquisition channel and sampled at 250 kHz, this allows the observation of the evolution of the emittance along the linac pulse. The diameter and the material of the wires are chosen in order to reduce the thermal effects induced by the beam and provide an adequate signal.

In order to sample both transverse planes two slits and two SEM-grids are needed. (see Fig. 3)

Figure 3: The emittance meter of LINAC4.

MULTIPLE SCATTERING AND THERMAL EFFECTS ON THE SLIT

Particles scattered on the edges of the slit could perturb the measurement of the distributions and lead to errors in the calculation of the emittance. The geometry of the slit and its material must be carefully selected in order to minimize this effect.

The effect of multiple scattering on the edges has been simulated for the four slit geometries shown in Fig. 4 and for different energies using the FLUKA Monte-Carlo code [2].

05 Beam Profile and Optical Monitors

Table 1: Simulation of Slit Efficiency at 3 MeV in Different Materials

	Carbon	Copper	Titanium	Steel	Aluminium
% particles after the slit	8.5	8.7	8.9	8.39	8.95
% scattered	6,29	3,98	5,85	3,91	6,731
% scatt. and hitting the SEM-grid	4,14	1,1	2,39	0,94	3,22

The results for a beam of 3 MeV and for the geometry indicated in Fig. 4-a are shown in Table 1. The simulations show that for the mentioned case less than 4% of particles collected by the SEM-grid are scattered on the edges of the slit.
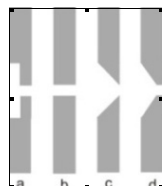

Figure 4: Different slit geometries used in the simulation. Each slit has an aperture of 100 μm and a maximum thickness of 1 mm.

The range of H⁻ ions in copper and stainless steel is shorter than the range in the lower Z materials while the scattering angle is larger; for this reason using higher Z materials reduces the fraction of the ions reaching the SEM-grid after interacting with the edges.

Comparisons of the different geometries shown in Fig. 4 in the case of stainless steel show that geometry (d) gives results similar to geometry (a), geometry (b) gives the best results and geometry (c) gives the worse results, with about 30% of the particles that reach the SEM-grid being scattered. It is important to note that geometry (b) is not well suited for sampling the phase-space. In this configuration the aperture of the slit is smaller than its thickness and the selection operated by the slit is no longer just in position, but also in angle. The result is that the measured phase-space distribution is flowed by an angular cut and the emittance is underestimated.

As FLUKA does not allow tracking particle below 100 keV in order to study the case of 45 keV simulations with beam energies of 200 kev and 300 keV have been used. For these two cases less than 0.01% of the particles passing through the slit are scattered on the slit edges. This result is due to the fact that the particles hitting the slit are stopped over a very short distance inside the material and as consequence only a very small fraction is able to escape. At 45 keV, the range of the H⁻ ions in steel is even shorter, so a similar result can be expected.

The energy deposition in the slit and the corresponding increase of temperature for the 3 MeV case have been also simulated with FLUKA showing that the increase in temperature exceeds the limits of stainless steel if the full beam intensity (400 μs) is sent on the slit.

In this case the maximum temperature increase is about 1500°C, which is above the melting point. For a shorter pulse of 200 μs the maximum increase of temperature

remains acceptable, around 750°C, further studies are needed in order to understand the effects of the 1 Hz repetition rate.

Table 2: Maximum Temperature Increase on the Slit

Beam energy	45 keV		3 MeV	
pulse	200 μs	400 μs	200 μs	400 μs
Stainless steel	11.2°C	22.6°C	760°C	1512°C
Carbon	29.25°C	58°C	2100°C	4000°C

SECONDARY EMISSION

The signals from the wires have several components:
- secondary emission (SE) caused by the H⁻ ions entering the wire
- secondary emission caused by protons and electrons exiting the wire
- direct charge deposition of protons and electrons stopped inside the wire

The SE signal can be calculated using the theory of Sternglaas [3]. In this theory the Secondary Emission Yield (SEY) is described as

$$SEY = \Lambda * dE/dx$$

where Λ is a parameter that depends on the properties of the material and dE/dx is the stopping power for the given material and particle type.

Measurements of the stripping cross section for H⁻ and H⁰ on carbon at 2 MeV and 7 Mev are available in literature [4]. The ionization cross sections depend on $\frac{1}{\beta^2}$ (relativistic factor) of the ions and on the Z of the material. In order to obtain values suitable for our studies the experimental results are interpolated using the mentioned dependencies, see Table 3.

Table 3: Measured and Extrapolated Ionization cross Sections

Stripping H⁻ in a H atom		
Beam Energy	Experimental cross section	Calculated cross section
2 MeV	$1 \cdot 10^{-16} cm^2$	
3 MeV		$0.66 \cdot 10^{-16} cm^2$
7 MeV	$0.35 \cdot 10^{-16} cm^2$	
12 MeV		$0.26 \cdot 10^{-16} cm^2$

Stripping H⁰ in a H⁺ ions		
Beam Energy	Experimental cross section	Calculated cross section
2 MeV	$0.4 \cdot 10^{-16} cm^2$	
3 MeV		$0.264 \cdot 10^{-16} cm^2$
7 MeV	$0.15 \cdot 10^{-16} cm^2$	
12 MeV		$0.11 \cdot 10^{-16} cm^2$

05 Beam Profile and Optical Monitors

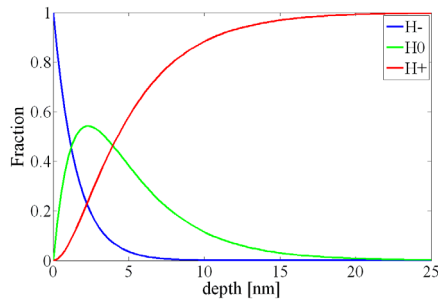Figure 5 shows the ratio of the different hydrogen ions mixture as a function of the depth inside a carbon foil.

Figure 5: Relative fraction of hydrogen ions inside a carbon foil for a 3 MeV impinging H⁻ beam.

The secondary emission is an effect that takes place in a very thin layer near the surface of the material. Below a few MeV the H⁻ ions are stripped in the first few nanometers and the secondary emission of the incoming particle is dominated by the proton while for beam energies above 3 MeV the ionization happens after the SE layer and the secondary emission is dominated by the H⁻ ions. The SEY of the H⁻ ions is again calculated with the Sternglass formula assuming that the stopping power of the H⁻ ions is the same as that of protons.

The secondary emission of the exiting particles depends on the ions energy and on the wire properties and geometry as the H⁻ ions will be decomposed into the 3 constituents and these will lose energy and eventually be stopped inside the material.

SIGNALS

An example of the evolution of the signal induced by H⁻ ions on a 40 μm wire (carbon and tungsten) as a function of the H⁻ energy is shown in Fig. 6.

At very low energies, the SE is the dominant source for the signal, and it shows a strong dependency on the ions energy as expected from the theory.

Above a few MeV the SE is much reduced and the signal is dominated by the direct charge deposition of the stopped electrons, becoming thus negative. Increasing further the energy of the ions, the two electrons acquire sufficient energy to cross the wires; at this point the secondary emission becomes again the dominant effect, but this time with a much smaller yield. In this case the SE of both the proton and of the electrons exiting the wire has to be considered. For a carbon wire of 40 μm in diameter, the threshold energy for the electrons crossing the wire is around 110 MeV. When crossing this threshold the signal drops to much smaller amplitudes. In the case of tungsten the transition happens around 160 MeV which corresponds to the maximum energy of LINAC4.

As for the slit, the energy deposition on the wires and the corresponding increase of temperature has been studied using FLUKA. As most of the particles are stopped by the slit, only 0.05% of the initial particles are transmitted through it, the total energy deposited in the

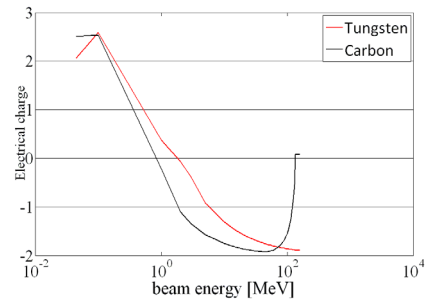wires is very small and the increase in temperature, even in the worst case, is only of about 20°C (tungsten).

Figure 6: Electrical charge induced on a 40 μm wire by H⁻ ions as function of the ions energy.

CONCLUSION

Monte Carlo simulations of the LINAC4 emittance meter have been performed in order to study the efficiency of the slit and estimate the thermal loads and the amplitude of signals from secondary emission. The results for a beam of 3 MeV show that by choosing an adequate geometry the multiple scattering on the slit edges will not perturb the sampling of the phase-space. A thermal analysis shows that the slit will be damaged if the full beam intensity is sent on it and thus the emittance must be measured using a shorter beam pulse. The thermal load induced by the beam on the wires and the consequent increase in temperature is very small, well below the threshold for thermionic emission and far away from the limits of the material chosen for the wires.

Further simulations are being produced for beams of 12 MeV and higher, in order to design suitable slits for higher energies.

REFERENCES

[1] Linac4 technical design report, CERN-AB-2006-084 ABP/RF.

[2] FLUKA official website ww.fluka.org.

[3] E.J. Sternglass, Theory of Secondary Electron Emission by High-Speed Ions, Phys.Rev. 108(1957) 1.

[4] A. S. Artemov, Yu. K. Baigachev, A. K. Gevorkov and A. O. Sidorin, Zh. Tekh. Fiz. 68, 102–105 (August 1998).